

Search for Sub-threshold Photoproduction of J/ψ Mesons

P. Bosted,¹ J. Dunne,² C. A. Lee,³ P. Junnarkar,² M. Strikman,⁴ J. Arrington,⁵
 R. Asaturyan,⁶ F. Benmokhtar,⁷ M.E. Christy,⁸ E. Chudakov,¹ B. Clasie,⁹
 S. H. Connell,¹⁰ M. M. Dalton,³ A. Daniel,¹¹ D. Day,¹² D. Dutta,² R. Ent,¹
 N. Fomin,¹² D. Gaskell,¹ T. Horn,^{7,1} N. Kalantarians,¹¹ C.E. Keppel,⁸
 D.G. Meekins,¹ H. Mkrtchyan,⁶ T. Navasardyan,⁶ J. Roche,¹ V. M. Rodriguez,^{11,13}
 D. Kiselev (nee Rohe),^{14,15} J. Seely,⁹ K. Slifer,^{12,16} S. Tajima,¹² G. Testa,¹⁴
 Roman Trojer,¹⁴ F.R. Wesselmann,¹⁷ S.A. Wood,¹ and X.C. Zheng¹²

¹*Thomas Jefferson National Accelerator Facility, Newport News, Virginia 23606*

²*Mississippi State University, Mississippi State, Mississippi 39762*

³*University of the Witwatersrand, Johannesburg, South Africa*

⁴*University of Pennsylvania, University Park, PA 16802*

⁵*Physics Division, Argonne National Laboratory, Argonne, Illinois 60439*

⁶*Yerevan Physics Institute, Yerevan, Armenia*

⁷*University of Maryland, College Park, Maryland 20742*

⁸*Hampton University, Hampton, Virginia 23668*

⁹*Massachusetts Institute of Technology, Cambridge, Massachusetts, 02139*

¹⁰*University of Johannesburg, Johannesburg, South Africa*

¹¹*University of Houston, Houston, TX 77204*

¹²*University of Virginia, Charlottesville, Virginia 22904*

¹³*Universidad Metropolitana, San Juan, PR 00928*

¹⁴*University of Basel, Basel, Switzerland*

¹⁵*Paul Scherrer Institut, Switzerland*

¹⁶*University of New Hampshire, Durham, New Hampshire 03824*

¹⁷*Norfolk State University, Norfolk, Virginia, 23504*

(Dated: October 25, 2021)

Abstract

A search was made for sub-threshold J/ψ production from a carbon target using a mixed real and quasi-real Bremsstrahlung photon beam with an endpoint energy of 5.76 GeV. No events were observed, which is consistent with predictions assuming quasi-free production. The results place limits on exotic mechanisms that strongly enhance quasi-free production.

PACS numbers: 13.60.Le,14.40.Gx,25.20.Lj

I. INTRODUCTION

One of the main goals of nuclear physics is to understand to what extent a nucleus differs from a loosely bound system of quasi-independent nucleons. When nucleons are very close spatially, corresponding to rare high momentum components of the single particle wave function, many interesting and potentially exotic configurations can arise. One way to look for such configurations is with reactions that are significantly sub-threshold to production from a free nucleon. Of all such reactions, photoproduction of charmonium is one of the cleanest because the charm quark content of a nucleon is expected to be small compared to the light quarks. In light meson photoproduction, the quark content of the mesons can originate in the nuclear target, while in the case of charmonium photoproduction, the quark-interchange mechanism is essentially absent, and the reaction must proceed via gluon exchange in order for color to be conserved. In addition, the heavy mass of the charm quark (about 1.5 GeV) ensures a hard scale to the problem, making it more tractable in QCD.

A. Kinematics of sub-threshold photoproduction

The goal of this experiment was to study the production mechanisms in the extreme conditions of matter that may be relevant in heavy ion collisions. These conditions are ensured by using a photon beam energy well below photoproduction threshold on a free nucleon. In the quasi-free picture where a photon interacts with a single off-shell nucleon in a nucleus, the nucleon three-momentum \vec{P}_m must be pointing anti-parallel to the photon direction (z) for the invariant mass of the photon-nucleon system s to be above the threshold value of $(m + M_j)^2 = 16.3 \text{ GeV}^2$, where m is the nucleon mass and M_j is the J/ψ mass. An additional constraint is that the missing energy E_m cannot be too high. Specifically, we calculated s for a given photon energy k using

$$s = (k + m - E_m)^2 - k^2 - P_m^2 - 2\vec{k} \cdot \vec{P}_m. \quad (1)$$

From Eq. 1, it is clear that larger values of E_m correspond to smaller values of s , for fixed values of P_m . The highest value of E_m that is kinematically allowed is shown as a function of the magnitude of \vec{P}_m for photon energies of 4, 5, 6, and 8 GeV in Fig. 1 (for the case of \vec{P}_m anti-parallel to the photon direction). Since E_m must be greater than zero, this leads to the conclusion that for J/ψ photoproduction, the minimum nucleon momentum P_m increases

as the photon energy decreases. In particular the minimum momentum for 4 GeV photons is 1.15 GeV, for 6 GeV photons it is 0.35 GeV, and for 8 GeV photons it is 0.05 GeV. As discussed below, it is generally thought that the region where few-nucleon short-range correlations, hidden color configurations, and other short-range effects play a significant role for momenta larger than 0.35 GeV [1], corresponding to a photon energy of 6 GeV. This was therefore chosen as the ideal energy for the present experiment. In practice, we used a slightly lower energy due to accelerator limitations at the time that the data were taken.

Another way to realize the importance of short-range correlations comes from the observation that the photon threshold to produce J/ψ meson is 5.7 GeV for a deuteron target at rest, and 4.8 GeV for a triton or ^3He target. Thus, two-nucleon and particularly three-nucleon correlations in the carbon nucleus are needed to kinematically permit J/ψ photoproduction with photons with energies below 6 GeV. In the language of light-front (infinite momentum frame) QCD, photon energies of 4, 6, and 8 GeV correspond to minimal light-cone fractions $\alpha_{LC} = 2.2, 1.4,$ and 1.0 respectively, where $\alpha_{LC} = 1 - (E_m - P_{mz})/m$. In the limit of very large quark masses the cross section of onium production in the impulse approximation is expressed through the light-cone density matrix of the nucleus as s in Eq. 1 is $\approx k\alpha_{LC}m$. For the J/ψ case constraints due to the recoil mass contribute as well.

The kinematics of the present experiment (represented by the open circles in Fig. 1) all lie in the range $1.5 < \alpha_{LC} < 2$, corresponding to the region of multi-nucleon correlations [2]. The recoil effects in these kinematics essentially remove the contribution of two-nucleon short range correlations, as in this case the recoil energy is taken by one nucleon (this is the kinematic domain which was studied in recent Jlab experiments using the $(e, e'NN)$ reaction [3] and inclusive scattering [4] at $1 < x < 2$). The dominant contribution originates from the region where at least two nucleons balance the struck nucleon momentum, i.e. three or more nucleon correlations, which were studied so far only in $x > 2$ measurements [5].

B. The high \vec{P}_m region

The high \vec{P}_m momentum region is where few-nucleon short-range correlations are known to be important [6, 7], potentially leading to significantly enhanced yields compared to a simple quasi-free model. In the hard-scattering picture [1], this could correspond to strong contributions of twist 3-gluon exchange, compared to the minimal 2-gluon exchange needed

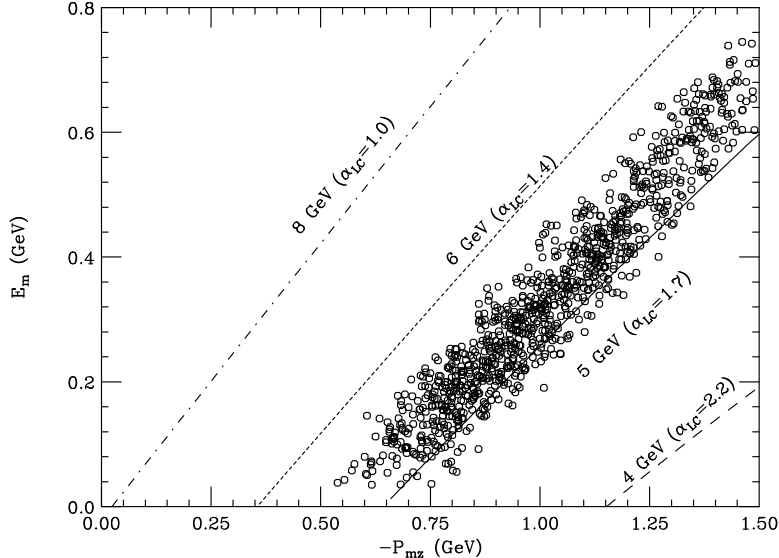


FIG. 1: The four curves show the maximum value of missing energy E_m as a function of the negative z component of missing momentum P_m , for 4, 5, 6, and 8 GeV photons, for the case of quasi-free photoproduction of J/ψ mesons from a nucleon bound in a nucleus. The circles represent the relative distribution of events predicted for the present experiment for the specific model described in the text [although no events were actually observed]. The values of light cone fraction α_{LC} are indicated for each photon energy.

to ensure the J/ψ color singlet final state. The influence of intrinsic charm contributions, or hidden color contributions, could potentially increase the cross section by an order of magnitude above the expectations of a quasi-free model (see Fig. 5 of Ref. [1]). Another possibility to enhance the sub-threshold cross section is a diagram in which two gluons are exchanged to two different nucleons. This type of process could become important in the sub-threshold region, because each of the gluons could have a much lower momentum fraction than if the pair of gluons came from a single nucleon.

C. Relation to sub-threshold hadroproduction

In pA collisions, it has been observed that anti-protons and kaons are produced on nuclear targets at substantially lower energies than is kinematically possible on free nucleons [8]. Scattering on a single nucleon in the nucleus would, at these energies, require a single-nucleon momentum in the vicinity of 800 MeV. While the pA data can be fit assuming

such high momenta are sufficiently likely, this assumption leads to an underestimate of sub-threshold production in AA collisions by about three orders of magnitude [9].

There are at least two qualitatively different scenarios for the observed sub-threshold production of anti-protons [10]. One scenario is that the projectile strikes a local “hot spot” with a high energy density in the nucleus. The effective mass of the scatterer is high, lowering the kinematic threshold. Alternatively, the momentum required to create the anti-proton is not transferred locally, but picked up in an extended longitudinal region. Establishing either scenario would teach us something qualitatively new about rare, highly excited modes of the nucleus.

Sub-threshold photoproduction can help to identify the correct mechanism, because the $c\bar{c}$ component of the photon is almost point-like at the charm threshold and below. Effects due to the shrinking effective size of a hadron probe near threshold are eliminated. The $c\bar{c}$ pair is created locally, within a proper time $\tau \simeq 1/m_c$. The extended acceleration scenario is thus not effective for charm photoproduction. If significant sub-threshold charm photoproduction occurs (beyond what can be ascribed to the quasi-free model) this selects the hot spot scenario.

II. QUASI-FREE MODELING

To model quasi-free photoproduction from a heavy nucleus, we use a convolution integral similar to the model for the deuteron described in Ref. [1]

$$d\sigma = \int \Phi(k) dk \int \frac{d\sigma_0(s, t)}{dt} \alpha_{LC}(P_m, E_m) S(E_m, \vec{P}_m) d^3\vec{P}_m dE_m dt \quad (2)$$

where the integral over nucleon momentum \vec{P}_m and energy E_m is limited to the kinematically allowed region, as described above, and the photon-nucleon center of mass energy squared s and momentum transfered t are functions of E_m , \vec{P}_m , and photon energy k . The elementary amplitude is far off shell (p^2 for the interacting nucleon is $\ll m^2$), which may lead of a significant suppression of the cross section, not taken into account in the present analysis. The photon flux $\Phi(k)$ is given by a/k , where a in the present experiment is the sum of the target thickness in radiation lengths divided by two, and an effective quasi-real electroproduction factor [11] of 0.02. The cross section $d\sigma_0(s, t)/dt$ is for J/ψ photoproduction from a free nucleon, and we assume for simplicity that neutron and proton cross sections are equal. The

flux term [2]

$$\alpha_{LC}(P_m, E_m) = \left(1 - \frac{E_m}{m} - \frac{\vec{k} \cdot \vec{P}_m}{km}\right) \quad (3)$$

averages to about 1.7 for the kinematics of this experiment (see Fig. 1). The function $S(E_m, \vec{P}_m)$ is a carbon spectral function [12]. The spectral function is defined as the probability of finding a nucleon of momentum \vec{P}_m and separation energy E_m in the nucleus. In this picture, the only unknowns are the model for $d\sigma_0(s, t)/dt$ and the carbon spectral function at high \vec{P}_m and E_m .

III. EXISTING DATA AND MODELS NEAR THRESHOLD

There are no published data on sub-threshold photoproduction, but it is useful to review the existing data just above threshold on a free nucleon, as this provides the baseline for sub-threshold predictions. The existing data below 20 GeV come from Cornell [13] using 9.3 to 11.8 GeV photons, and from SLAC [14] from 13 to 21 GeV. These experiments detected lepton pairs from the J/ψ decay to provide relatively background-free measurements. Additional unpublished data from SLAC [15] detected only a single lepton, leading to relatively large background subtractions.

The experiments typically parameterize the data according to $d\sigma/dt = Ae^{bt}$. What is remarkable is that, while b has values of 3 to 5 GeV^{-2} at high energy, which are characteristic of diffractive processes, the values drop rapidly near threshold, with Cornell [13] quoting a value of only $1.25 \pm 0.2 \text{ GeV}^{-2}$ for an 11 GeV photon energy. It was pointed out by Ref. [16], the actual slope of the data seems to be more like 1.5 GeV^{-2} , still quite small. The Cornell value is more than a factor of two below the SLAC value of $b = 2.9 \pm 0.3 \text{ GeV}^{-2}$ at 19 GeV. It is difficult to reconcile the two experiments with a smooth fit, assuming the exponential form corresponds to an effective form factor. One way to resolve this is to assume that $d\sigma/dt$ scales as a dipole form factor squared of the form $(1 - t/m_0^2)^{-4}$ [16]. A reasonably good fit to all data up to photon energies of 100 GeV can be found with $m_0^2 \approx 1 \text{ GeV}^2$. Since each experiment measured over a limited range of t , and $-t_{min}$ increases near threshold, a natural explanation for the variation of b with photon energy can be found. We found a reasonable dipole fit to the low energy data is given by $d\sigma/dt = 2.5/(1 - t)^4 \text{ nb/GeV}^2$, where t is in units of GeV^2 . In the QCD picture of Laget [1], this almost flat dependence on photon energy corresponds to three-gluon exchange dominance, while 2-gluon exchange

should have an extra factor of $(1 - x)^2$, where x is the momentum fraction. In the definition of Ref. [1], $x = ((m + M_J)^2 - m^2)/(s - m^2)$ is unity for at the threshold for photoproduction. In the approach of Ref. [16], a different definition of x is used which yields a maximum value of about 0.8, so factors such as $(1 - x)^2$ do not cause a large threshold suppression.

In summary, there is a very large uncertainty in how to extend fits to existing free-nucleon cross section measurements below 11 GeV. This is discussed in more detail below in the context of cross section limits from the present experiment.

IV. EXPERIMENT

The experiment was performed in 2004 in Hall C at the Thomas Jefferson National Accelerator facility (JLab). The layout of the spectrometers and detectors is indicated in Fig. 2.

A. Beam and target

The J/ψ search data taking used a 5.76 GeV continuous-wave (CW) electron beam with a typical current of 60 μA , and lasted for eight days. The integrated beam charge on target was 27 Coulombs. The electron beam impinged on a narrow solid ^{12}C target with a thickness (in the beam direction) of 2.5 gm/cm^2 , or 0.06 radiation length (r.l.). The effective photon flux per electron was $0.05 dk/k$, where k is the photon energy, obtained by considering that on average half of the real photons produced in the target are usable, plus an effective 2% from small-angle electroproduction.

B. Spectrometers and detectors

The experiment used the High Momentum Spectrometer (HMS) in coincidence with the Short Orbit Spectrometer (SOS) to measure lepton pairs from J/ψ decays (6% branching ratio for each of e^+e^- and $\mu^+\mu^-$). The magnets of the HMS were configured to detect positive charged particles while the SOS had negative polarity. The HMS central momentum was set at 3.5 GeV/c and the central scattering angle at 24 degrees. The SOS had a central momentum set near its maximum value of 1.7 GeV/c and the central angle set to 53

degrees. These settings were chosen to optimize the acceptance for forward-angle J/ψ mesons decaying to lepton pairs, with the assumption that the angular distribution of the lepton pairs is given by $1 + \cos^2(\theta_{cm})$ [17], where θ_{cm} is the center-of-mass (c.m.) decay angle. The optimization was done assuming the elementary cross section model had the form $d\sigma/dt = 2.5/(1 - t)^4$ nb/GeV² and the spectral function of Benhar [12] (with one of the high P_m extrapolations discussed below) to generate a sample of quasi-free J/ψ mesons. The choice of spectrometer polarities was made to minimize backgrounds and random coincidences. The CW nature of the electron beam was essential to reducing accidental coincidences to an acceptable level.

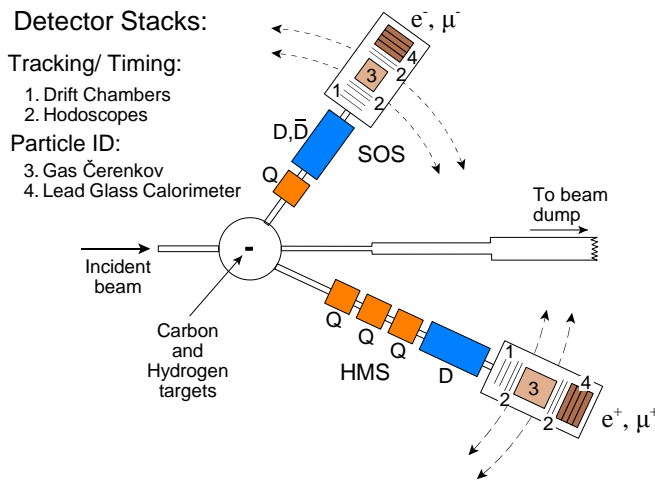


FIG. 2: (color online) Layout of spectrometers and detectors, where Q and D represent quadrupole and dipole magnets respectively.

C. Particle identification

Electrons in the SOS and positrons in the HMS were identified by requiring a signal of several photoelectrons in threshold gas Cherenkov counters, with the threshold momentum for pions or heavier particles to produce Cherenkov light set above the maximum accepted particle momentum in the given spectrometer. In addition, at least 70% (90%) of the particle energy was required to be deposited in an array of lead glass blocks in the SOS (HMS). These cuts reduced contamination from other particles to a negligible level, while preserving an efficiency of over 90% of electron-positron pairs.

Separating muons from pions was more problematic. In the case of the HMS spectrometer,

the pion threshold in the gas Cherenkov counter was set just below the maximum accepted momentum (i.e., about 8% above the central momentum). The threshold for muons was 25% lower than for pions, and therefore 17% below the central momentum of the spectrometer (which has a nominal momentum acceptance of $\pm 10\%$). With approximately 10 photo-electrons (PE) for fully relativistic particles (such as electrons), the muons produced on average 2 PE to 4 PE over the spectrometer acceptance. With a threshold of 1 PE, the efficiency was varied from 85% to 98%, depending on muon momentum. The original Cherenkov counter in the SOS was designed to be sub-atmospheric, hence could not achieve the correct index of refraction to trigger on muons. It was therefore replaced with the SLAC 1.6 GeV spectrometer Cherenkov counter modified for the scattered particle envelope in the SOS. This detector was filled with C_4F_{10} and was pressurized to trigger on muons, but not on pions. Additional muon identification was provided by requiring minimum ionizing pulse heights in each of the four layers of the lead glass shower counters. The overall efficiency for muon pairs was estimated to be 80%.

Drift chambers in each spectrometer were used to measure particle momenta with a resolution of better than 0.2%, and scattering angles with an accuracy of 1 to 3 mr. The resulting resolution on the di-lepton mass is approximately 10 MeV. Scintillator paddles in each spectrometer were used for triggering, background rejection, and additional particle identification. The last two features are illustrated in Fig. 3, which shows the number of events as a function of δt , the time difference between the SOS and HMS relative to that expected for di-lepton pairs (the time difference between electron-positron and di-muon pairs is negligible on the scale used). The top panel (Fig. 3a) is for the case of a cleanly identified electron in the SOS, and all events in the HMS (dominated by protons and pions). The peak near zero is due to pions, and the peak near -4 ns is due to protons. The observed peak widths are about 0.5 ns (1σ). The random accidental background is very small.

D. Di-lepton events

The electron-positron time difference spectrum is plotted in Fig. 3b. Only one event is observed in the cut region $-1.5 < \delta t < 1.5$ ns (illustrated as the vertical dashed lines), and there are no events in the electron-proton or accidental coincidence regions. The di-muon time difference spectrum is plotted in Fig. 3c. Only one event is observed in the cut region

$-1.5 < \delta t < 1.5$ ns but in this case there are 26 events in the lepton-proton peak region. The latter are due to protons that produced a signal in the Cherenkov counter (either from knock-on electrons, or from scintillation light). A few accidental-in-time events are also visible.

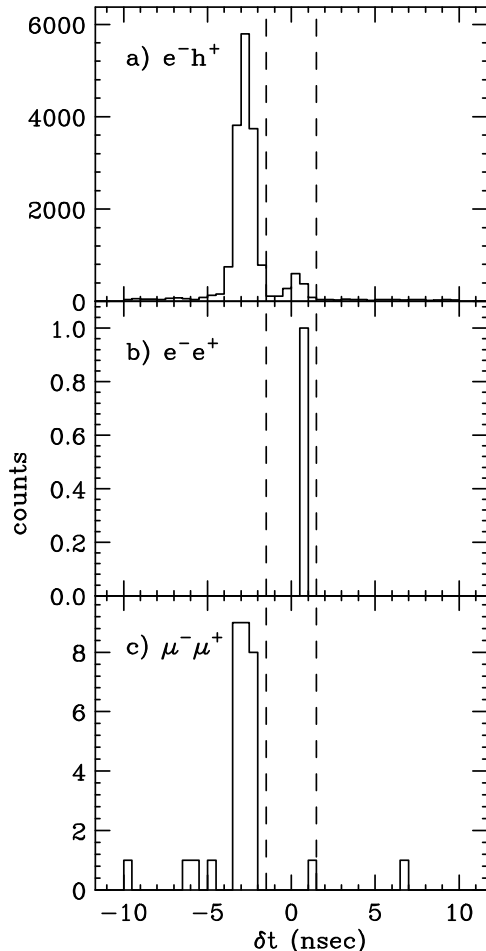


FIG. 3: Time difference spectra between the HMS and SOS spectrometers, relative to that expected for di-lepton events, for: a) electrons in the SOS and any particle in the HMS; b) electrons in the SOS and positrons in the HMS; c) muons in both the SOS and the HMS.

After putting a cut around the time-difference peaks shown in Fig. 3, the reconstructed mass spectra using the HMS and SOS particles (M_{ll}) was determined and are shown in Fig. 4. For electron-pion coincidences, shown in Fig. 4a, the mass spectrum is smooth, and covers the mass range $2.5 < M_{ll} < 3.5$ GeV. This basically illustrates the phase space acceptance of the two spectrometers, and shows good acceptance at the J/ψ mass of 3.097 GeV. As illustrated in Fig. 4b, the one coincident e^+/e^- event has an invariant mass of

only 2.71 ± 0.01 GeV, more than 40σ from the J/ψ mass. Thus this event is background: either an electron-pion event (with the pion mis-identified as a positron), or a wide-angle pair conversion of a Bremsstrahlung photon. As illustrated in Fig. 4c, the one coincident μ^+/μ^- event has an invariant mass of only 2.87 ± 0.01 GeV, more than 30σ from the J/ψ mass. Thus this event is also background: mostly likely an accidental coincidence, but it could also be a wide-angle pair conversion of a Bremsstrahlung photon or a process involving particle mis-identification, or the decay of pions to muons.

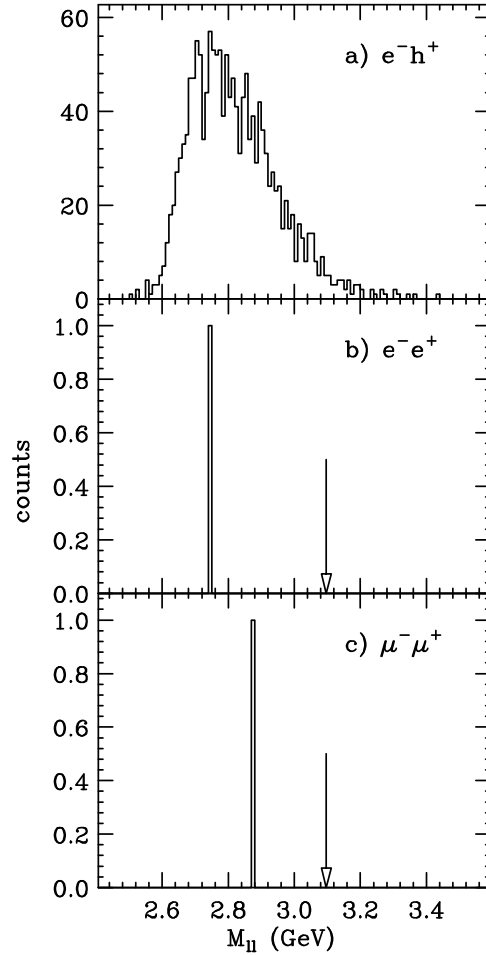


FIG. 4: Invariant mass spectrum from a negative particle in the SOS, and a positive particle in the HMS, for events passing the timing cuts shown in Fig. 3. The arrows correspond to the J/ψ mass.

TABLE I: Calculated probability of detecting a di-lepton pair from J/ψ decay in this experiment at the indicated values of J/ψ momentum P and lab angle θ with respect to the beam direction. The results are scaled by 10^6 and averaged over e^+/e^- and μ^+/μ^- pairs.

P (GeV)	$\theta = 0.4^\circ$	1.2°	2.0°	2.8°	3.6°	4.4°	5.2°	6.0°	6.8°
5.81	0	0	2	4	0	2	4	0	0
3.95	78	58	84	76	44	30	24	8	5
4.09	344	317	276	242	172	102	42	12	8
4.23	617	580	516	446	186	97	44	16	10
4.37	478	440	394	337	243	91	48	12	6
4.51	190	222	226	210	164	129	74	16	4
4.65	8	26	51	63	82	48	26	16	2
4.79	0	0	4	4	6	2	2	0	0

E. J/ψ Acceptance

In order to facilitate the calculation of the predicted number of events for a given sub-threshold cross section model, we give here the J/ψ acceptance corresponding to the HMS and SOS setting used in this experiment. This was determined by a detailed Monte Carlo simulation of the spectrometers, convoluted with the di-lepton decays of J/ψ mesons with a particular momentum and polar angle with respect to the beam axis. The results are shown in Table I, and indicate a maximum detection probability of about 0.5×10^{-4} for momenta near 4.3 GeV and angles less than 3 degrees.

F. Calibration Runs

Several calibration runs were performed to check the kinematic settings and verify that the spectrometers were fully functional. The first calibration check was to set up the spectrometers for coincident $p(e, e', h)X$ running where h could be either a positively-charged pion, proton, or kaon. A liquid hydrogen target replaced the carbon target and the HMS was moved forward to 13 degrees. Three SOS angles were used, 53° , 40° , and 27° . These central kinematics corresponded to four momentum transfers of $Q^2 = 7.8, 4.6, \text{ and } 2.1 \text{ GeV}^2$, and

invariant mass $W = 0.8, 2.0,$ and 2.5 GeV, respectively. In all cases, the peaks in the missing mass spectra were at the proper positions and the widths were understood. As an example, using proton cuts on the HMS arm, the missing mass spectrum for $p(e, e', p)X$ shows prominent η and π^0 peaks at the correct locations (as seen in previous Hall C experiments [18]). As a further check of the luminosity, accidental and multi-pion continuum backgrounds were subtracted from the data to produce experimental yields. These yields were corrected for radiative effects and spectrometer acceptances to produce differential cross sections. Good agreement was found between the measured and simulated differential cross sections [18]. This indicates that the target density and electron beam current determinations were well understood.

The other significant calibration check was to set the spectrometers to measure lepton pair decays from other lower mass vector mesons. In particular, we centered the spectrometers to detect e^-/e^+ pairs from ω and ρ meson decays. For these runs a beryllium target was used with the SOS set to 25 degrees and a central momentum of 0.9 GeV, and the HMS set to 11 degrees and a central momentum of 1.95 GeV. In spite of the very small branching ratios of about 0.5×10^{-5} , a clear $\omega(785)$ peak with the expected full width of 8 MeV was seen on top of a 140 MeV wide $\rho(770)$ peak, as illustrated in Fig. 5. The number of detected ω events is consistent with the predicted number from a Monte Carlo simulation that had as much as possible in common with the simulation of J/ψ events.

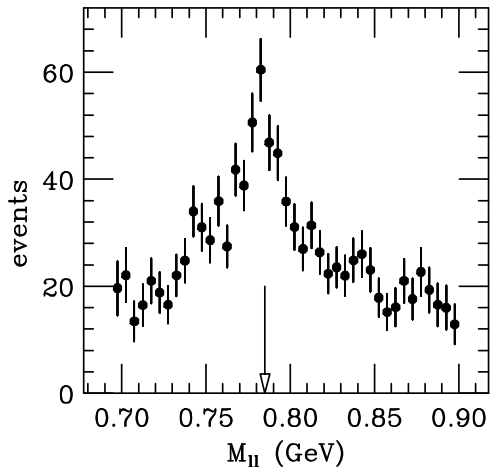


FIG. 5: Acceptance-corrected invariant mass spectrum from an electron in the SOS and a positron in the HMS, at kinematics optimized for detection of $\omega(785) \rightarrow e^+e^-$ (indicated by arrow) and $\rho(770) \rightarrow e^+e^-$.

V. RESULTS

Since no J/ψ mesons were detected in this experiment, here we try to quantify what the implications are for elementary photoproduction cross section models, in the context of the single-particle convolution model described above, for four choices of the prescription used to extend the spectral function of Benhar [12] beyond $P_m = 0.6$ GeV (where there is insufficient data from $C(e, e'p)X$ to constrain the function). We show two “eyeball” extrapolations of the probability distribution integrated over E_m in Fig. 6. We label this as “high” and “low” according whether they are higher or lower at large P_m . As it happens, these extrapolations are quite similar to the two extrapolations (for nuclear matter) shown in Fig. 1 of Ref. [6]. As discussed in Ref. [6], the “high” extrapolation should probably be considered as an upper limit, and probably will over-estimate yield predictions. We used two choices for the E_m distribution: a) “freeze” the E_m distribution to that of Benhar et al. [12] at $P_m = 0.8$ GeV (the highest provided in this fit); b) shift the E_m distribution by $\sqrt{m^2 + P_m^2} - \sqrt{m^2 + 0.8^2}$, with P_m in units of GeV. The latter corresponds to following the “ridge” observed at lower E_m . Using the nuclear matter prescription of Eq. 10 in Ref. [6] should give results somewhere between these two cases, as their prescription involves shifting the E_m distribution along the same “ridge”, but having the width increase with increasing P_m . Following Ref. [2], we also investigated scaling the spectral function by a relativistic correction factor $m/(m - E_m)$ and found the results to change by less than 20%.

We used three different free nucleon cross sections (as motivated by the discussion in the introduction):

$$\text{I. } d\sigma/dt = ae^{bt} \quad (4)$$

$$\text{II. } d\sigma/dt = a/(1 - bt)^4 \quad (5)$$

$$\text{III. } d\sigma/dt = a(1 - x)^2/(1 - bt)^4, \quad (6)$$

where a and b are free parameters, and we used $x = ((m + M_J)^2 - m^2)/(s - m^2)$. For each model, we varied the t -slope parameter b within a reasonable range and, for each value of b , determined a such that the total cross section would agree with the Cornell measurement [13] of 0.7 nb at $k = 11$ GeV. The predicted counts are shown in Fig. 7 as a function of b for each of the three models for four high- P_m extrapolations of the spectral function. The predictions for model III are quite a bit lower than models I and II, due to the factor of $(1 - x)^2$. The

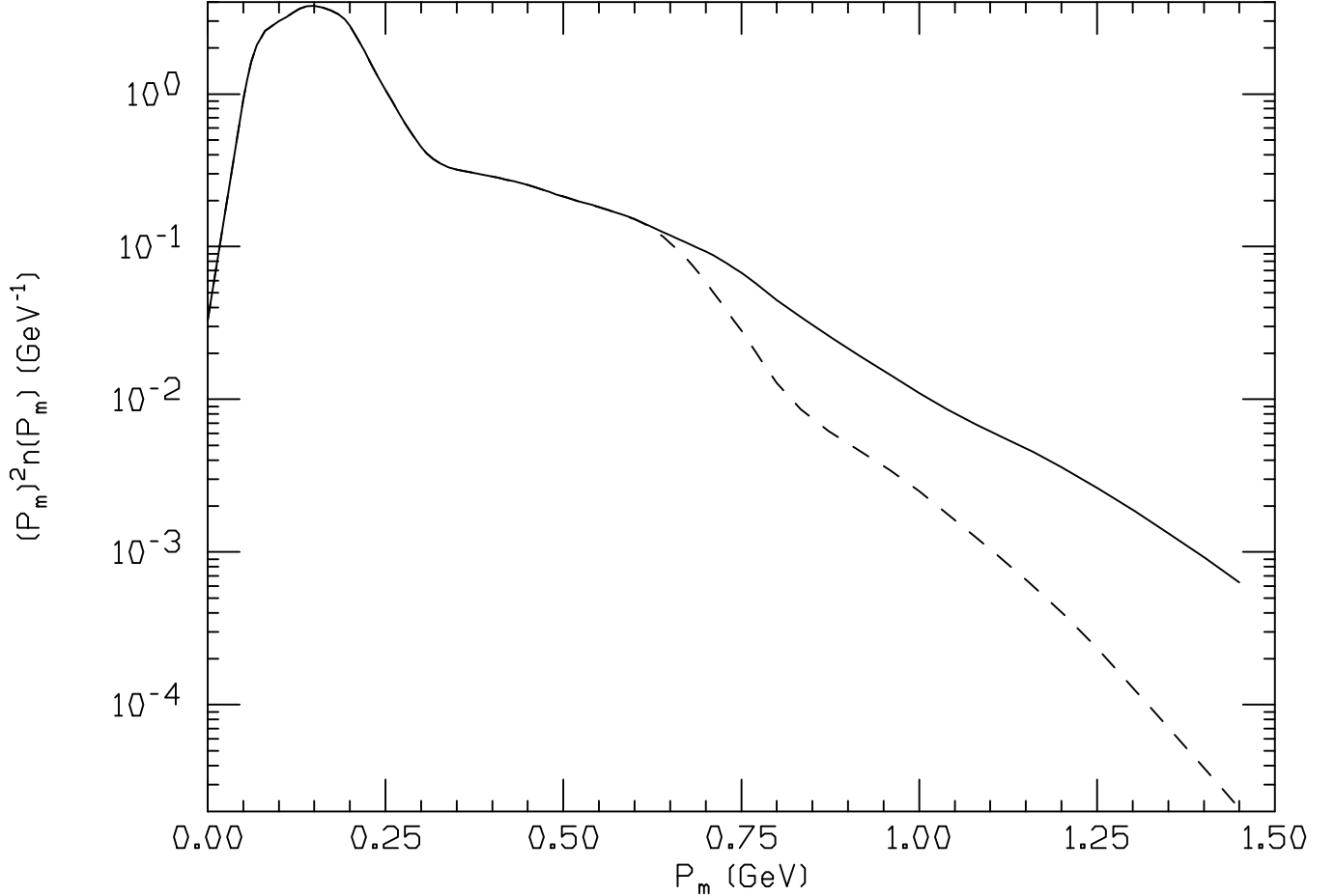


FIG. 6: The E_m -integrated probability of finding a nucleon with missing momentum P_m as a function of P_m . The solid (dashed) lines are “high” and “low” eyeball extrapolations above 0.6 GeV of the spectral function of Ref. [12].

sensitivity to the spectral function extrapolation is also largest for model III, because on average higher values of P_m are probed. For all models, “shifting” the E_m distributions for $P_m > 0.8$ GeV makes a difference of typically a factor of two in predicted rates. Not shown in the figure is the effect of assuming $E_m = P_m^2/2(A-1)m$ (i.e., a virtual photon interacting with an almost on-shell nucleon), as was initially assumed in the planning phase of the present experiment. This assumption results in predicted rates higher by approximately two orders of magnitude than if a more realistic E_m distribution is used.

While the predicted number of counts is below our 87% confidence level observation of less than 2 counts (shown as the hatched bands in Fig. 7) for all the combinations considered here, it is not impossible that for some cross sections models (I and II in particular), something

like the “hot spot” scenario discussed in the introduction could result in a prediction of more than two counts. In the quasi-free picture, this could correspond to considerably lower average values of E_m than in the Benhar spectral function.

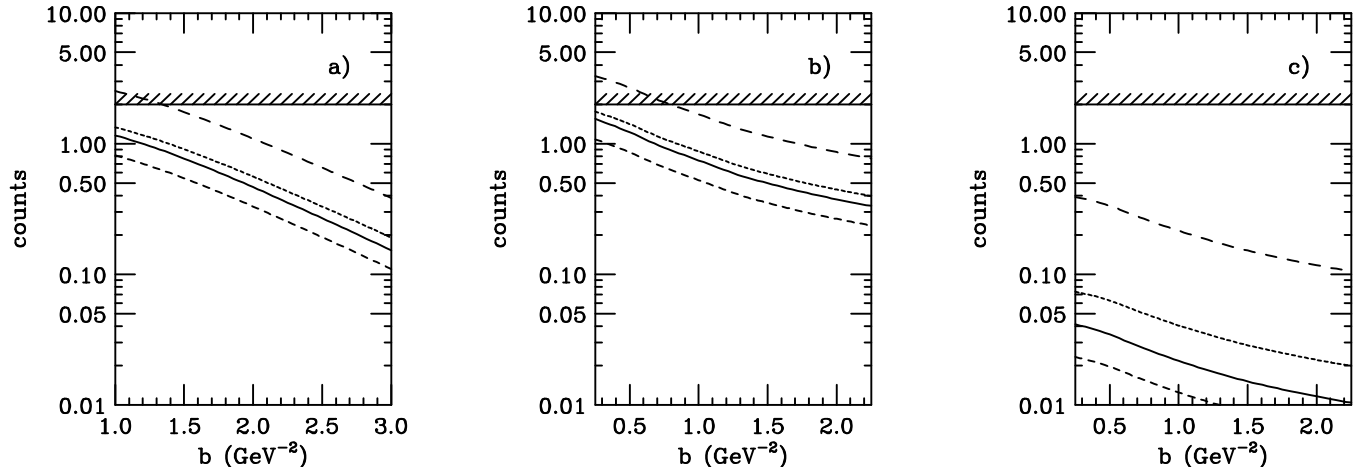


FIG. 7: The number of predicted counts for the conditions of the present experiment as a function of b for: a) Model I; b) Model II; and c) Model III, where the models are defined in Equations 4, 5, and 6, respectively. On each panel, the solid (long dashed) curves use the “high” extrapolation of the spectral function (see Fig. 6) with (without) the E_m shift for $P_m > 0.8$ GeV described in the text. The medium dashed (short dashed) are the corresponding curves with the “low” extrapolation. The hatched band at 2 counts indicates the 87% confidence level corresponding to our experimental observation of no events.

While we are not aware of any detailed theoretical predictions for sub-threshold J/ψ photoproduction specifically, we can use the calculation of charm ($C\bar{C}$) photoproduction of Braun and Vlahovic [19] as a possible guide. Using pQCD to evaluate the photon-gluon fusion process, they predict a total cross section of 0.25 fb/nucleon for carbon for 5.5 GeV photons. This corresponds to approximately 0.02 events for our experimental conditions. This is similar to our predictions using Model III.

VI. CONCLUSION

The non-observation of sub-threshold J/ψ photoproduction on carbon in the present experiment is consistent with predictions of quasi-free production with a variety of reasonable

elementary free nucleon cross sections models near threshold, and educated guesses for the high missing momentum and missing energy spectral function distributions in carbon. For a given set of assumptions on the cross section and spectral function choices, upper limits could be set on exotic mechanisms that could potentially enhance the sub-threshold cross sections (such as gluon exchange to two different nucleons, hidden color configurations, 3-gluon exchange, etc.). The interpretation of the present experiment will be greatly aided with precision measurement of the elementary free nucleon cross section near threshold, planned at Jefferson Lab [20] once beam energies up to 11 GeV are available.

The authors wish to thank J.M. Laget for theoretical support. This work is supported in part by research grants from the U.S. Department of Energy and the U.S. National Science Foundation. The South African group acknowledges the support of the National Research Foundation. The Southeastern Universities Research Association operates the Thomas Jefferson National Accelerator Facility under the U.S. Department of Energy contract DEAC05-84ER40150.

-
- [1] S.J. Brodsky, E. Chudakov, P. Hoyer, and J.M. Laget. Phys. Lett. **B498**, 23 (2001).
 - [2] L. L. Frankfurt and M. I. Strikman, Phys. Lett. **B183**, 254 (1987).
 - [3] R. Shneor *et al.*, [Jefferson Lab Hall A Collaboration], Phys. Rev. Lett. **99**, 072501 (2007); Science **320**, 1476 (2008).
 - [4] K. S. Egiyan *et al.*, [CLAS Collaboration], Phys. Rev. Lett. **96**, 082501 (2006).
 - [5] K. S. Egiyan *et al.*, [CLAS Collaboration], Phys. Rev. C **68**, 014313 (2003).
 - [6] O. Benhar, S. Fantoni, and G.I. Lykasov, Eur. Phys. J. **A5**, 137 (1999).
 - [7] L. L. Frankfurt and M. I. Strikman, Phys. Rep. **160**, 236 (1988).
 - [8] J. B. Carroll *et al.*, Phys. Rev. Lett. **62**, 1829 (1989).
 - [9] A. Shor, V. Perez- Mendez and K. Ganezer, Nucl. Phys. **A514**, 717 (1990).
 - [10] P. Hoyer, Nucl. Phys. **A622**, 284C (1997).
 - [11] R.H. Dalitz and D.R. Yennie, Phys. Rev. **105**, 1598 (1957).
 - [12] O. Benhar, A. Fabrocini, S. Fantoni, and I. Sick, Nucl. Phys. **A579**, 493 (1994).
 - [13] B. Gittelman *et al.*, Phys. Rev. Lett. **35**, 1616 (1975).
 - [14] U. Camerini, *et al.* Phys. Rev. Lett. **35**, 483 (1975).

- [15] R. Prepost, Report SLAC-R-191, p. 267 (1975); SLAC-PUB-1689 (1975).
- [16] L. Frankfurt and M. Strikman, Phys. Rev. D **66**, 031502 (2002).
- [17] K. Schilling, P. Seyboth, G. E. Wolf, Nucl. Phys. **B15**, 397 (1994).
- [18] M.M. Dalton *et al.*, arXiv:0804.3509.
- [19] M.A. Braun and B. Vlahovic, Phys. Lett. **B594**, 105 (2004).
- [20] Jefferson Lab E12-07-106, P. Bosted, E. Chudakov, and J. Dunne, co-spokespersons.